Rhizosphere bacterial characteristics reveal the invasive advantage of Sphagneticola trilobata compared to the greening grass Axonopus compressus

Guixiang Li
Hainan Normal University
Xin Liu
Hainan Normal University
Mingzhao Han
Hainan Normal University
Xiao Qin
Hainan Normal University
Peng Li
bio_lip@hainnu.edu.cn

Hainan Normal University

Research Article

Keywords: ecological balance, microbe-plant interplay, weed invasion, rhizosphere microbiome

Posted Date: September 30th, 2025

DOI: https://doi.org/10.21203/rs.3.rs-7532857/v1

Additional Declarations: No competing interests reported.

Version of Record: A version of this preprint was published at BMC Microbiology on February 10th, 2026.
See the published version at https://doi.org/10.1186/s12866-026-04817-y.

Rhizosphere bacterial characteristics reveal the invasive advantage of *Sphagneticola trilobata* compared to the greening grass *Axonopus compressus*

Guixiang Li, Xin Liu, Mingzhao Han, Xiao Qin, Peng Li*

Ministry of Education Key Laboratory for Ecology of Tropical Islands, Key Laboratory of Tropical Animal and Plant Ecology of Hainan Province, College of Life Sciences, Hainan Normal University, Haikou 571158, China

***Address correspondence to Peng Li, Email: bio_lip@hainnu.edu.cn**

ORCID

Guixiang Li: 0009-0000-7009-6157

Xin Liu: 0009-0007-8728-6054

Mingzhao Han: 0000-0001-7427-4053

Xiao Qin: 0009-0008-2718-6366

Peng Li: 0000-0002-1906-8393

Abstract

Background: Due to the excellent invasive ability, the plant *Sphagneticola trilobata* poses a severe threat to local ecosystems. We hypothesized that its invasive success is highly related to its ability of shaping a beneficial rhizosphere microbiome. To test this, we compared the rhizosphere bacterial communities of *S. trilobata* (SRS) and a common greening grass *Axonopus compressus* (ARS).

Result: We found that *S. trilobata* cultivates a significantly more diverse and structurally distinct bacterial community, enriched with key taxa (Rhizobiales, Cytophagales, Pseudomonadaceae, Comamonadaceae, and *Novosphingobium*) that are known as the groups associated with nitrogen fixation and plant growth promotion, and exhibited a more complex and cooperative interaction network than ARS. Functional predictions indicated an enhanced capacity for lipid and carbohydrate metabolism in SRS, suggesting efficient nutrient cycling around its rhizosphere. Crucially, a synthetic community (SynCom) constructed from SRS-enriched bacteria promoted the biomass of *S. trilobata* significantly and altered resource allocation towards roots under nutrient-poor conditions.

Conclusion: Our findings provide strong evidence that *S. trilobata* engineers a specialized rhizosphere microbiome that confers direct competitive advantage compared with other local plants, revealing a key microbial mechanism underlying its successful invasion.

Keywords: ecological balance; microbe-plant interplay; weed invasion; rhizosphere microbiome

Background

Globalization and increasing anthropogenic activities have made invasive plants one of the most pressing challenges to global ecosystems [1]. By competing for resources, altering soil properties, and disrupting the ecological niches of native species, the invasive plants could impact biodiversity and ecology balance significantly. Together with the typically characterized by robust ecological adaptability and high reproductive capability, which enable them to outcompete native species for resources. Additionally,

they can influence the growth of other plants by releasing allelochemicals, which have been demonstrated to affect soil enzyme activity and alter the composition of soil microbial communities [2]. These changes potentially lead to alterations in soil nutrient cycling. Meanwhile, the altered microbial activity, driven by allelochemicals, affects plant interactions, cycling and availability of nutrients in the soil, ultimately reshaping ecosystem structure and function [3,4]. Extensive studies have demonstrated that invasive plants such as *Solidago canadensis* L. and *Conyza canadensis* L. can significantly inhibit the growth of native plant species and facilitate their invasion by releasing allelochemicals [5-7]. Further scientific evidence indicates that allelochemicals induce changes in microbial communities, triggering significant responses in functional genes, particularly those associated with carbohydrate metabolism, nitrogen fixation, ammonia oxidation, nitrite reduction, and phosphate transport [8]. These microbial shifts may influence nutrient cycling in soil and affect nutrient acquisition by plants, playing a key role in the formation of plant communities.

The rhizosphere is a crucial ecosystem where interactions occur among plant roots, soil microorganisms, minerals, and organic matter interact, collectively influencing plant growth and development [9], as well as the role in regulating soil nutrient availability, modulating plant endogenous hormone signalling, and the suppressing pathogen proliferation [10]. Moreover, researches have also demonstrated that invasive plants can substantially increase soil microbial biomass and the abundance of harmful organisms, thereby enhancing soil microbial diversity [11,12]. For instance, *Mikania micrantha* has been shown to modify the composition of rhizosphere microbial communities via its root exudates, resulting in augmented soil microbial functional diversity, particularly in the rhizosphere [13]. Hence, these microbial alterations foster a soil micro-environment that favors the proliferation and propagation of invasive plants.

S. trilobata has invaded southern China extensively and is now exhibiting a trend of spreading towards the colder northern areas [14], and is designated as a Level 2 invasive

species (serious invaders requiring containment) in China [15]. Meanwhile, through the secretion of allelochemicals, which threatens local biodiversity and disrupts ecological balance greatly [16]. *Axonopus compressus*, an introduced species naturalized in southern China [17], owing to its tolerance for poor soils and trampling, which is widely utilized in parks, gardens, and lawns, and has become a major turfgrass across tropical and subtropical regions [18]. However, because of its ecological niche overlaps with that of *S. trilobata*, making it one of the primary species affected by the latter's invasion. Given the widespread invasion of *S. trilobata* in southern China, this study aims to explore its competitive advantages over *A. compressus* by examining rhizosphere bacterial diversity characteristics. Through an comparative analysis of soil bacterial community composition, we aim to elucidate the underlying mechanisms of the invasive success of *S. trilobata* and provide insights into its ecological impact on the microbial level.

Results

Quantitative characteristics of the bacterial community

The 16S rRNA amplicon sequencing of the 75 samples generated 451,019 raw sequences, and a total of 102,503 OTUs were identified. The bacterial community was classified into two domains (Bacteria and Archaea), encompassing 54 phyla, 164 classes, 412 orders, 654 families, 1,272 genera, 2,002 species and 31,172 OTUs (Suppl. Tab. 1). Analysis of the dilution curves (Fig. 1a) based on the Pielou evenness index showed that the curves plateaued as sequencing depth increased, which indicates that the sequencing data were sufficient to capture the majority of the bacterial diversity in the samples. Our results demonstrated that the SRS exhibited the highest Pielou index, suggesting the most even bacterial distribution, whereas CK had the lowest index, indicating the least uniform distribution. The other three soil types (SSS, ARS, ASS) showed intermediate values, with relatively similar evenness. Significant differences in OTU composition were also observed among the five plot types (Fig. 1b). Venn analysis identified 1,392, 1,365, 1,183, 1,316, and 1,241 unique OTUs in the samples SRS, SSS, ARS, ASS, and CK, respectively. These findings highlight the distinct bacterial community structures associated with different soil environments of different plants.

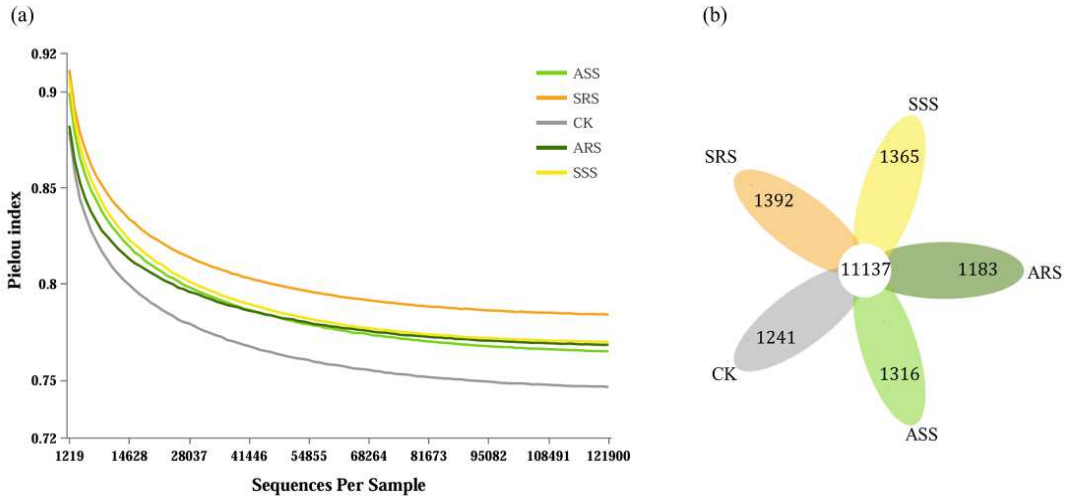

Fig. 1 Dilution curves among different soil types (a) and Venn analysis of shared and unique bacteria OTUs (b).

Beneficial bacterial taxa are specifically enriched in the *S. trilobata* rhizosphere

Analysis of the bacterial community composition at the phylum level revealed that Proteobacteria, Acidobacteriota, Chloroflexi, Bacteroidota, and Actinobacteria were the dominant phyla across all samples (Fig. 2a). A clear rhizosphere effect was observed, with the relative abundance of Proteobacteria and Bacteroidota increasing from bulk soil towards the rhizosphere of both plant species. Notably, this enrichment was more pronounced in SRS, where Proteobacteria reached 39.64% abundance, compared to 36.25% in ARS and 28.73% in CK. At the class level, Alphaproteobacteria, Gammaproteobacteria, Acidobacteriae, Bacteroidia, and Actinobacteria were the predominant groups, and the Bacteroidia exhibiting higher abundance near the rhizosphere (Fig. 2b). At the order level, Burkholderiales was the most abundant group, followed by Rhizobiales, Vicinamibacterales, Chthoniobacterales, and Sphingomonadales. Furthermore, the bacterial composition of SSS was more similar to SRS, while ASS was more similar to ARS, indicating distinct influences of the two plant species on soil bacterial communities (Fig. 2c).

To pinpoint the specific bacterial taxa that differentiate the rhizosphere microbiomes, we performed a Linear Discriminant Analysis Effect Size (LEfSe) analysis comparing

SRS and ARS (Fig. 3a). The analysis identified a suite of biomarkers significantly enriched in the *S. trilobata* rhizosphere. The SRS harbored nine key biomarkers (LDA > 3.5), including the orders Rhizobiales and Cytophagales, the families Pseudomonadaceae and Comamonadaceae, and the genus Novosphingobium (Fig. 3b). These taxa are well-known for their roles in crucial ecological functions such as nitrogen fixation, organic matter decomposition, plant growth promotion, and the degradation of allelochemicals. However, the ARS was characterized by only seven biomarkers, primarily belonging to the phylum Gemmatimonadota and the order Chloroflexales, which are often associated with oligotrophic or stress conditions. These results indicate that *S. trilobata* can shape and host a unique soil community actively, then lead to the significant enrichment of a functionally beneficial consortium of bacteria in its immediate root zone.

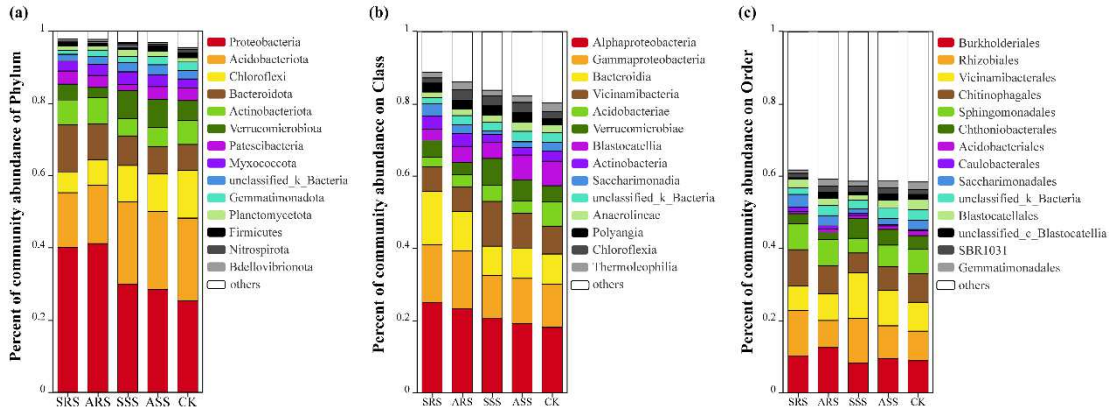

Fig. 2 Comparison of bacterial community abundance in different soil types on Phylum (a), Class (b), and Order (c) levels.

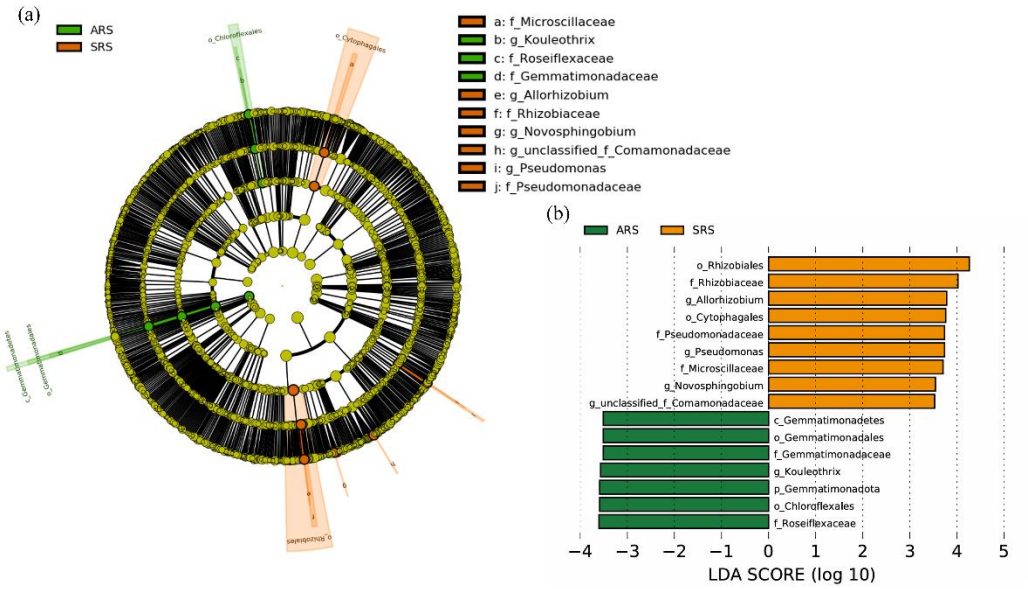

Fig. 3 LEfSe analysis (a) and LDA distribution (b) of different species in SRS and ARS.

The *S. trilobata* rhizosphere microbiome exhibits a distinct structure and higher diversity of rhizosphere bacterial community

Based on the compositional differences, we then further assessed the overall structure and diversity of the bacterial communities. Non-metric Multidimensional Scaling (NMDS) analysis supported a clear separation of bacterial communities according to sample type (Fig. 4a). The rhizosphere soil communities of SRS and ARS formed two distinct clusters, which were also well-separated from their surrounding soils (SSS and ASS) and the adjacent bulk soil (CK). Notably, the SRS samples clustered more tightly together than any other group, suggesting that *S. trilobata* consistently assembles a more stable and uniform microbial community across different sampling locations.

To further quantify the differences in community richness and evenness, we analyzed alpha diversity indices. The rhizosphere of *S. trilobata* (SRS) harbored a significantly richer bacterial community, as indicated by the highest Chao1 index among all groups ($p < 0.05$ vs. CK, Fig. 4b). Furthermore, the SRS community was also more diverse and evenly structured. It exhibited the highest Shannon index and the lowest Simpson index ($p < 0.05$ vs. CK), indicating a well-balanced community not dominated by a few taxa (Fig. 4c, 4d). The high Pielou's evenness index for SRS further corroborated this finding (Fig. 2a). In contrast, the alpha diversity indices for ARS were generally lower

than SRS and closer to those of the bulk soil, suggesting a less profound influence on the richness and evenness of its rhizosphere community.

The uniqueness of the SRS community was also evident at the OTU level. Venn diagram analysis showed that SRS contained the highest number of unique OTUs (1,392) among all plant-associated soil types (Fig. 2b).

In summary, these analyses demonstrate that the specific enrichment of taxa in the *S. trilobata* rhizosphere translates into a community that is structurally distinct, more stable, and possesses higher species richness and evenness compared to that of *A. compressus*.

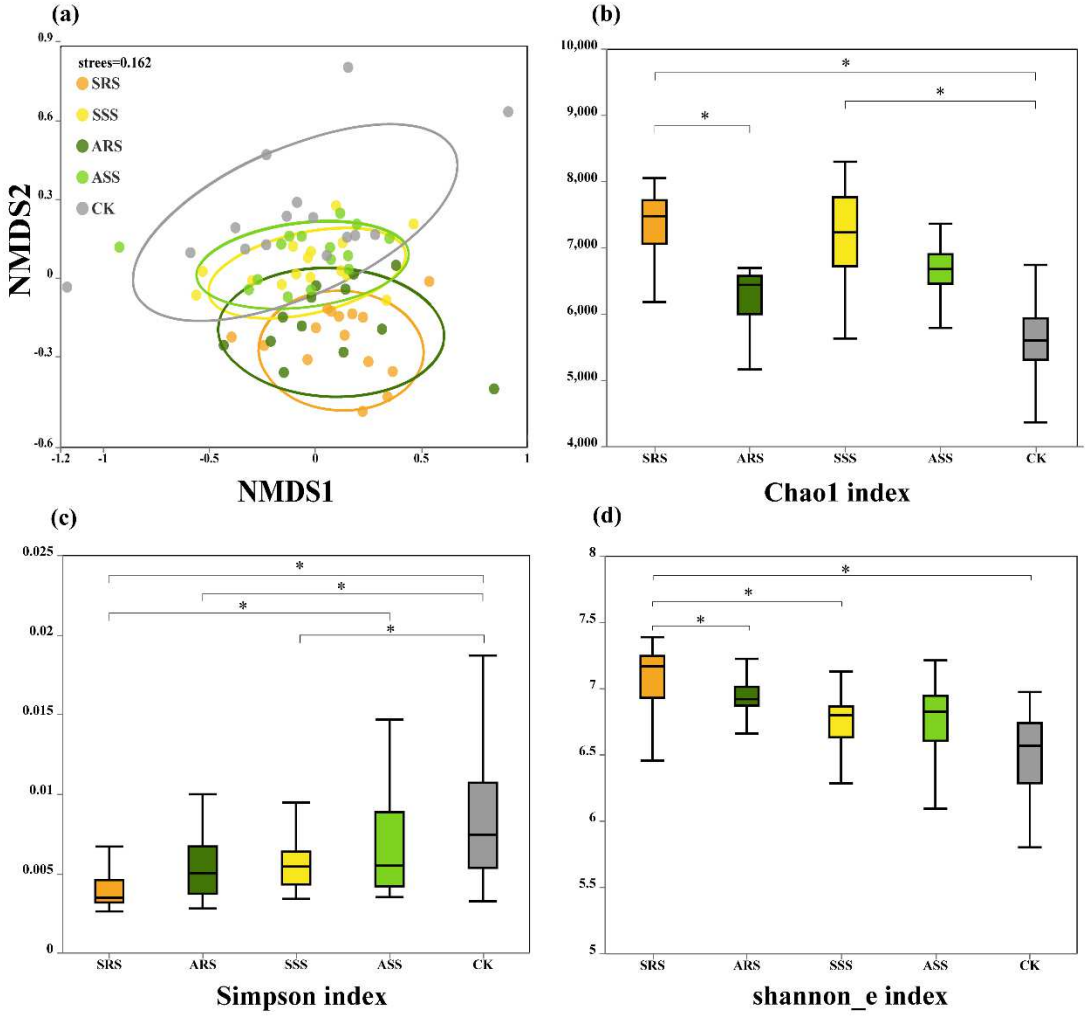

Fig. 4 Alpha and Beta diversity of bacteria community. (a) NMDS analysis of bacterial community (b) Chao1 index (c) Simpson index (d) Shannon index. "*" indicates a significant difference at the $p<0.05$.

The *S. trilobata* rhizosphere fosters a more complex and functionally robust microbial network

To reveal the symbiotic relationships among soil microorganisms, correlation network analysis was performed at the top 30 genus level. The soil from the *S. trilobata* area (SRS+SSS) displayed the highest network complexity (Fig. 5a): it possessed the greatest number of nodes, connections, and positive correlations, and harboured six keystone genus (each with >5 links). In contrast, the *A. compressus* soil (ARS+ASS) and the adjacent bulk soil (CK) formed markedly simpler networks with fewer nodes and a higher proportion of negative links (Fig. 5bc). This pattern indicates that the SRS bacterial community is more collaborative and stable, whereas competition or antagonism prevails in the other two soils.

Functional profiles were then predicted with the COG database. Cluster analysis of the ten most enriched functional genes showed that SRS and ARS grouped together, clearly separated from the non-rhizosphere soils (Fig. 6). Between the two rhizosphere soils, SRS exhibited a significant enrichment in carbohydrate transport and metabolism (G), whereas ARS was notably enriched for lipid transport and metabolism (I). These results suggest that the SRS community is geared toward efficient energy and material cycling, whereas the ARS community may experience environmental stress, given that lipid metabolism is often linked to stress signalling.

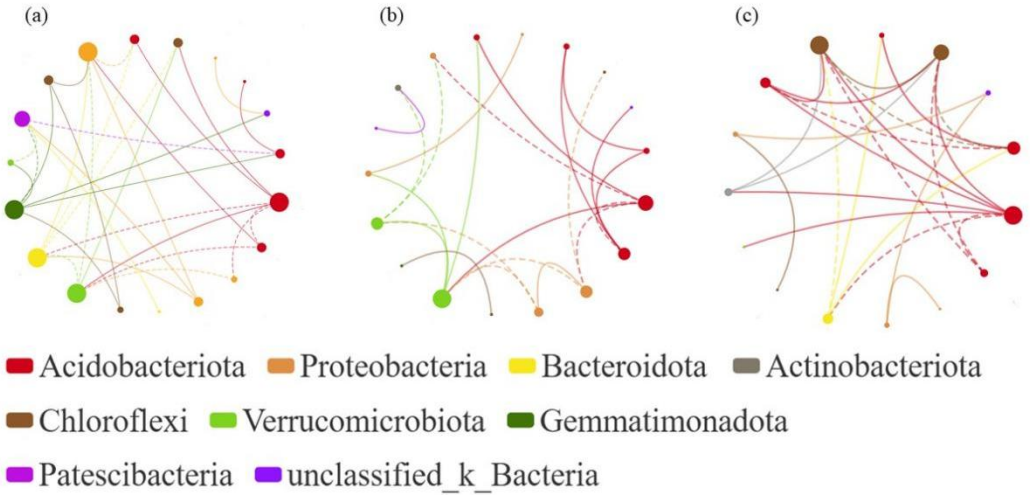

Fig. 5 Bacterial correlation networks in different soil types. (a) SRS+SSS; (b)

ARS+ASS; (c) CK. Nodes represent species, with the size of the node indicating the number of its connecting lines. Different colours represent different genus classifications at the phylum level, and the lines between nodes indicate correlations between orders, with solid lines representing positive correlations and dashed lines representing negative correlations.

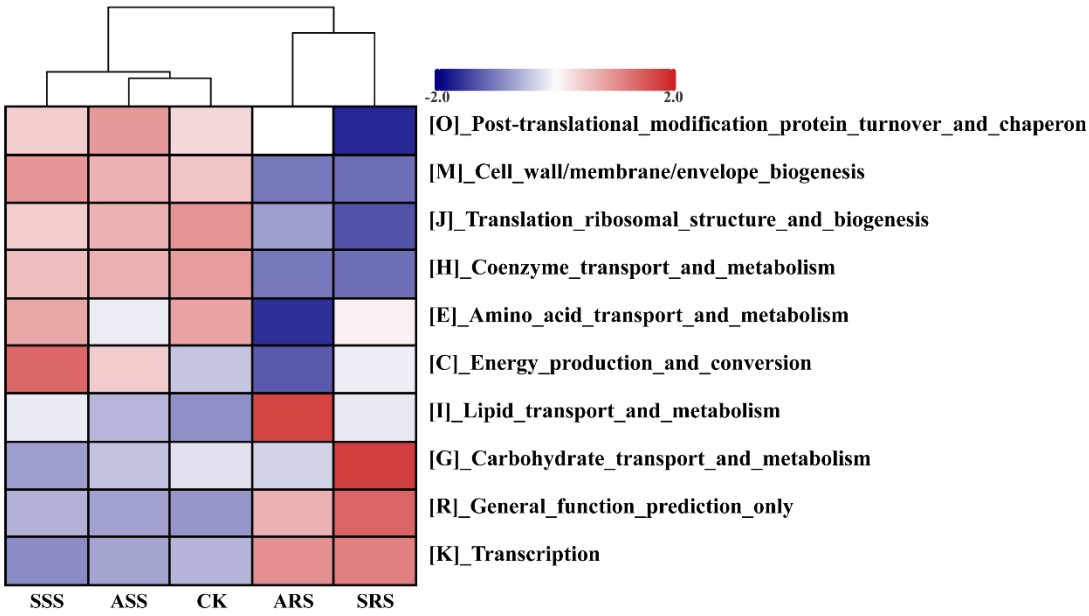

Fig. 6 Cluster analysis Heatmap of different soil types base on COG database. Heat-map colours represent centred and scaled relative abundances of each functional category; red indicates enrichment, blue indicates depletion.

A synthetic community of enriched taxa directly promotes *S. trilobata* growth

To evaluate the functional benefits of bacteria enriched in the *S. trilobata* rhizosphere, 68 cultivable isolates were obtained from its rhizosphere soil. Functional screening using Root extract (RE) identified one *Streptomyces* and three *Pseudomonas* strains that exhibited significantly enhanced growth in RE-supplemented medium compared with controls (Suppl. Fig. 1a-d; Suppl. Fig. 2). Interestingly, their taxnomic identities were consistent with bacterial groups enriched *S. trilobata* rhizosphere as revealed by amplicon sequencing (Suppl. Fig. 3). Thus, a synthetic microbial community (SynCom) composed of these four strains was subsequently established for inoculation

experiments under sterile nutrient-poor conditions.

Quantitative assessment of plant performance revealed significant treatment-dependent differences (Fig. 7; Fig. 8). Plants grown in feritile soil (FS) exhibited the highest biomass accumulation and growth, whereas those in infertile soil (IS) showed markedly reduced development across all measured parameters (Fig. 8 a,b,d,e). However, SynCom inoculation in nutrient-deficient soil substantially alleviated this growth suppression, leading to significantly higher biomass and root development compared with IS (Fig. 8 a,b,d,e). Moreover, SynCom treatment increased the root-to-shoot ratio compared to IS and FS (Fig. 8c), suggesting an adaptive shift in biomass allocation. In addition, the specific leaf area (SLA) was highest in IS plants, but significantly reduced by SynCom inoculation, approaching values observed in FS (Fig. 8f). Together, these results demonstrate that SynCom inoculation functionally beneficial for nutrient limitations by enhancing plant biomass production and improving resource allocation efficiency.

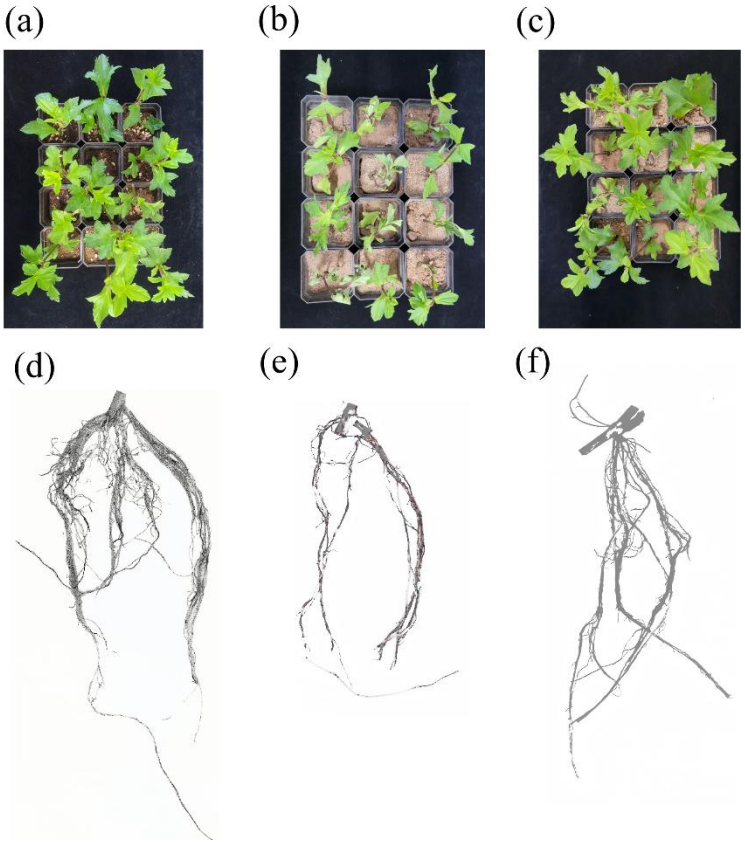

Fig. 7 Comparative morphology of *S. trilobata* under differential soil treatments. (a) FS

plants exhibiting vigorous shoot growth; (b) IS+SynCom plants showing moderate growth with leaf curling; (c) IS plants displaying stunted growth; (d) Extensive root system development in FS; (e) Underdeveloped root architecture in IS; (f) Moderately developed roots in IS+SynCom.

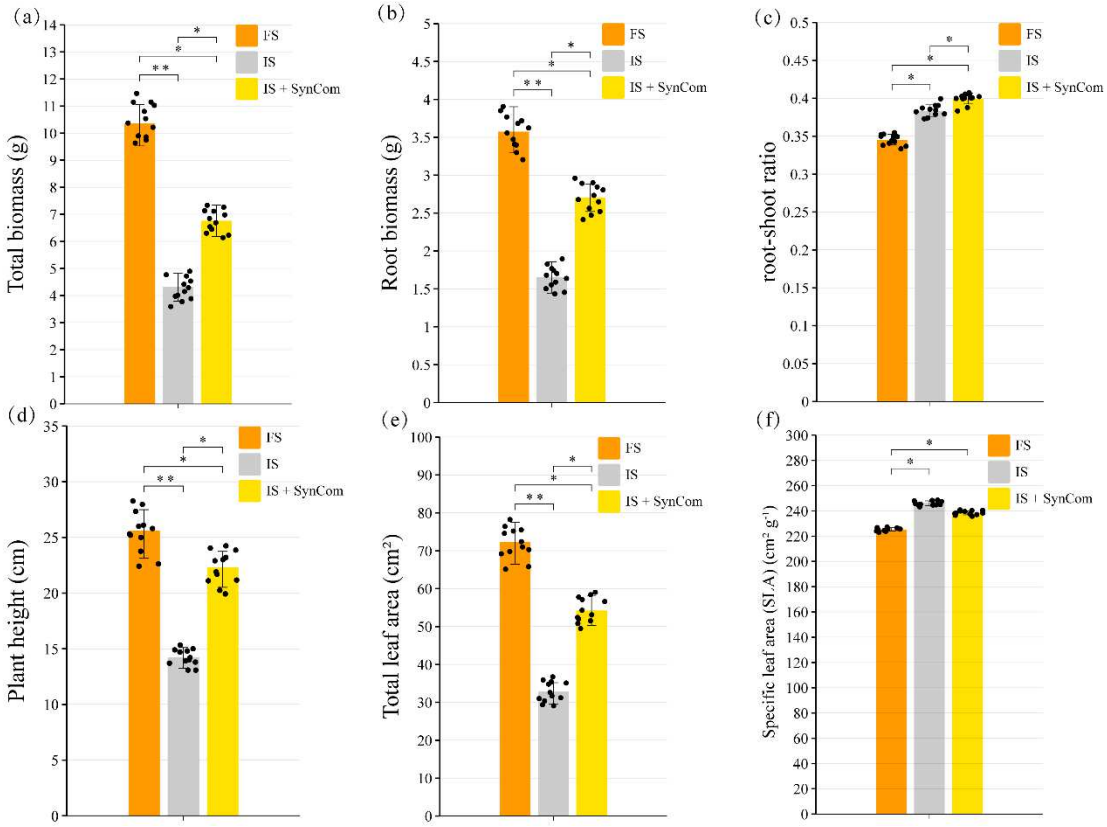

Fig. 8 Growth parameters of *S. trilobata* under differential soil treatments. (a) Total biomass; (b) Root biomass; (c) Root-shoot ratio; (d) Plant height; (e) Total leaf area; (f) Specific leaf area (SLA).

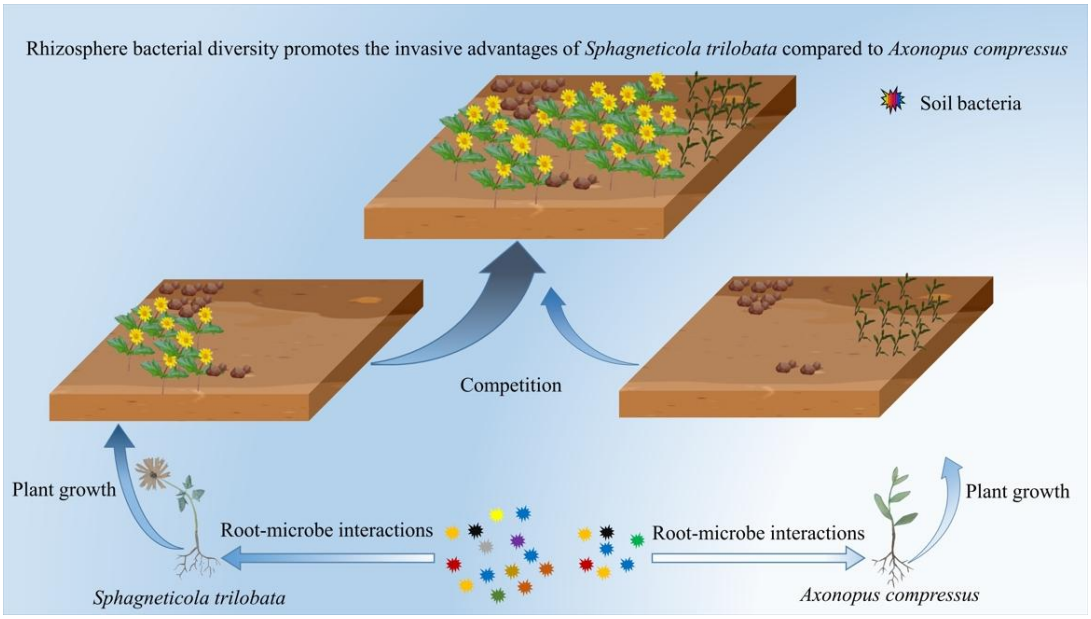

Fig. 9 The differences in root - microbe interactions between *S. trilobata* and *A. compressus*. The soil bacteria are represented by different colored dots, and the thickness of the arrows indicates the strength of the interactions.

Discussion

Differential bacterial community assembly in invasive and Naturalized plant rhizospheres

Due to its high ecological adaptability and reproductive capacity, *S.trilobata* has become a successful invader in southern China, severely threatening native biodiversity and ecosystem balance. Understanding its invasion mechanisms is essential for controlling its further spread. This study compared the rhizosphere microbiomes of *S. trilobat*a and the turfgrass *A. compressus*, revealing that the invader assembles specialized microbial communities which enhance its growth and competitive dominance. The contrasting root–microbe interactions of invasive plant *S. trilobata* and naturalized plants *A. compressus* illuminate a mechanistic basis for their competitive asymmetry (Fig. 9). SRS exhibited significantly higher Shannon diversity and greater community evenness (Pielou's index) than ARS (Fig. 1a; Fig. 4d), highlighting the capacity of *S. trilobata* to assemble a more diverse and balanced rhizosphere

285 microbiome. The dominance of Proteobacteria in SRS (Fig. 2a), which were positively
286 correlated with root proximity, implies active recruitment via root exudates. These taxa
287 contribute crucially to nitrogen cycling and soil fertility through nitrogen fixation,
288 denitrification, and organic matter decomposition [19,20], thereby directly enhancing
289 plant competitiveness. In contrast, Acidobacteria abundance declined toward roots,
290 likely due to rhizosphere alkalization driven by root exudates and respiration [21,22];
291 their highest levels in CK (Fig. 2a) also reflect the acidified soil background typical of
292 southern China [23]. LEfSe analysis further identified key functional groups enriched
293 in SRS (Fig. 4), including nitrogen-fixing Rhizobiales [24,25], allelochemical-
294 detoxifying Novosphingobium [26,27], and antifungal/growth-promoting
295 Pseudomonadaceae and Comamonadaceae [28,29]. Conversely, ARS was
296 characterized by biomarkers indicative of chronic stress, primarily drought-adapted
297 Gemmatimonadaceae and Chloroflexales (30-32). This contrast is ecologically
298 significant: the extensive root system and dense growth of *S. trilobata* (Suppl. Fig 4a)
299 enhance its ability to exploit subsurface water, thereby imposing hydraulic stress on
300 adjacent *A. compressus*, which exhibits lower vegetation cover and reduced root
301 biomass (Suppl. Fig 4b). Consequently, the enrichment of stress-tolerant taxa with
302 sporulation capacity and low metabolic rates in ARS reflects both niche partitioning
303 and the outcome of resource competition [33,34]. These findings collectively
304 demonstrate that *S. trilobata* shapes a beneficial rhizosphere microbiome that supports
305 nutrient acquisition and growth, whereas *A. compressus* harbors a stress-adapted
306 community, underscoring a key microbial mechanism underlying the invader's
307 competitive dominance.

308 **Community stability, networks and functional genes**

309 NMDS analysis revealed a tightly clustered and stable bacterial community in SRS (Fig.
310 4a), suggesting that *S. trilobata* consistently assembles a conserved core microbiome
311 across different microenvironments. This stability contrasts sharply with the dispersed
312 clustering of bulk soil (CK) communities, underscoring the strong host filtering effect
313 of the invasive plant. Further supporting this finding, co-occurrence network analysis
314 indicated that the SRS microbiome formed a more complex and interconnected network,

with a higher proportion of positive correlations and more keystone taxa (Fig. 5). Such topological features often indicate enhanced functional redundancy and resilience to environmental disturbance [35]. In contrast, the simpler, more antagonistic network observed in ARS and bulk soils implies a less cooperative and more stress-prone microbial community. Functional predictions via PICRUSt aligned with these structural differences, revealing a strategic functional partitioning between the two rhizospheres. The enrichment of genes related to carbohydrate transport and metabolism in SRS suggests a microbiome optimized for energy acquisition and carbon turnover, potentially supporting the high growth rates of *S. trilobata*. On the other hand, the significant enrichment of lipid metabolism pathways in ARS may indicate a stress-adapted response. Lipid metabolism is often upregulated under environmental challenge, serving as a component of signaling and membrane adaptation mechanisms under resource competition or osmotic stress [36].

Functional validation via synthetic community inoculation

Our SynCom experiment provides causal evidence that the SRS signature is functionally advantageous rather than merely correlative. Among them, the three *Pseudomonas* strains further overlapped with LEfSe indicators in SRS (Fig. 3) and occupied keystone positions in the network analysis (Fig. 5). Although *Streptomyces* was not an LEfSe indicator or network keystone, its abundance in SRS was 1.8–2.3× higher than in ARS or CK (Suppl. Fig 3b), justifying its inclusion as a "quantitative keystone" taxon with documented nitrogenase and antibiotic biosynthetic capacity [37]. When inoculated into sterile nutrient-poor substrate, the SynCom markedly enhanced host plant growth (Fig. 7). More notably, a profound shift in carbon allocation strategy was observed: SynCom-inoculated plants exhibited a significantly higher root-to-shoot ratio (Fig. 8c), reflecting a strategic investment belowground consistent with the "functional equilibrium" model, wherein plants prioritize root development when microbial symbionts improve nutrient availability [38]. Further supporting this metabolic reallocation, a reduction in specific leaf area (SLA) indicated thicker, more nitrogen-rich leaves—a trait associated with relieved nutrient stress and heightened photosynthetic efficiency [39]. This phenotypic response mirrors observations in other

systems where beneficial microbiota mitigate abiotic stress, such as in *Coffea arabica* under drought conditions following inoculation with ACC deaminase-producing bacteria [40].Taken together, these results demonstrate that *S. trilobata* not selectively recruits but also functionally leverages a specialized root microbiota that enhances nutrient assimilation, modulates host resource allocation, and ultimately confers a growth advantage in challenging environments—thereby facilitating its successful invasion.

Conclusion

The invasive advantage of *S. trilobata* over *A. compressus* is strongly linked to its ability to shape a more specialized and beneficial rhizosphere bacterial community. The rhizosphere microbiome of *S. trilobata* exhibited higher diversity, greater stability, and contained more keystone taxa involved in nutrient acquisition and allelochemical detoxification. In contrast, the rhizosphere of *A. compressus* supported a less complex microbial network with higher abundance of stress-adapted bacteria. Functional validation through synthetic community inoculation confirmed the growth-promoting effects of *S. trilobata*-enriched bacteria under nutrient-limited conditions. These results emphasize the importance of host-mediated microbiome assembly in enhancing plant fitness and invasion success, providing critical insights into the microbial mechanisms underlying plant invasions.

Methods

Research region

The was conducted at the Campus of Hainan Normal University, Haikou, Hainan, China (110.510048°E, 19.981393°N), which is characterized by a tropical monsoon climate. To account for the diversity of vegetation and the potential influence of human activities within the campus, 15 sampling sites were selected (Fig. 10). Each site was situated within the interspecific competition zone between *S. trilobata* and *A. compressus*. In addition, to provide a comparative basement, each sampling site included areas with sparse or minimal vegetation cover, referred to as adjacent bulk soil. No permits were required as both species are common, non-endemic and not protected under Chinese or

CITES regulations. Identification was carried out by Prof. Peng Li using the *The Checklist of the Alien Invasive Plants of China*. No voucher specimens were prepared.

Soil sampling

Five soil types were selected for this study: *S. trilobata* rhizosphere soil (SRS), *S. trilobata* surrounding soil (SSS), *A. compressus* rhizosphere soil (ARS), *A. compressus* surrounding soil (ASS), and adjacent bulk soil (CK). The large soil clumps adhering to plant roots were removed, and the plants samples were transported to ice box immediately and treated in the laboratory. Rhizosphere soil was collected by shaking the roots to remove the loose soil while the soil tightly adhering to the root surface were collected. Surrounding soil was collected from a depth of approximately 5-10 cm below the soil surface, with adjacent bulk soil sampled similarly from adjacent areas with no plants. Each soil type was sampled five times within the same region, and the collected samples were thoroughly mixed to form a composite sample. A total of 15 locations were studied, yielding 75 composite soil samples. All samples were stored at -80°C for further analysis. Additionally, the same rhizosphere soil was used for subsequent bacterial isolation aimed at constructing a synthetic community

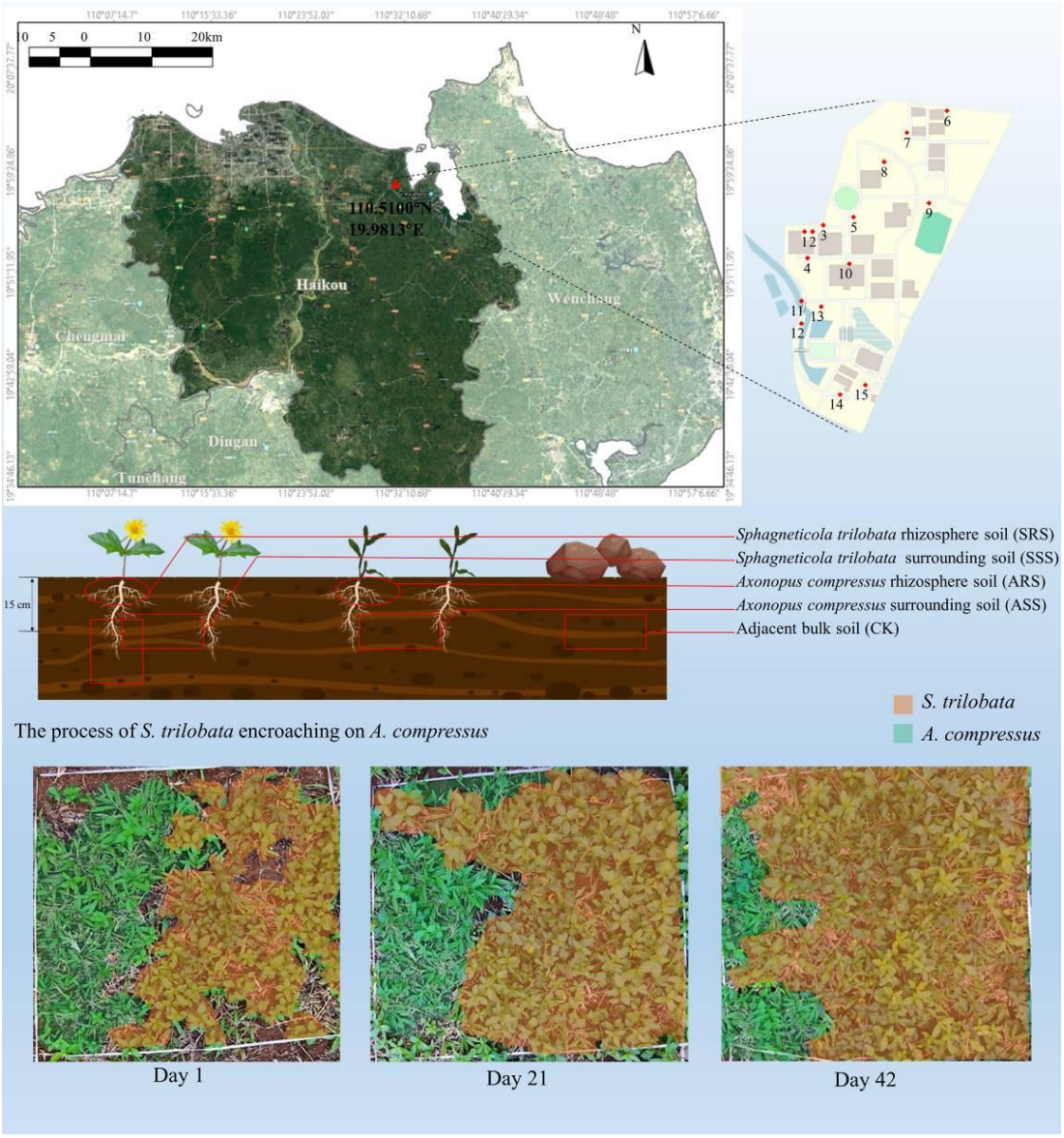

Fig. 10 Characteristics of soil structure and invasion process of *S. trilobata*.

DNA extraction and sequencing analysis

Genomic DNA was extracted from soil samples using the DC306 Magnetic Bead Soil DNA Extraction Kit (Ark Biosafety Technology Co., Ltd., Guangzhou, China) following the manufacturer's instructions. The integrity and purity of the extracted DNA were assessed via 1% agarose gel electrophoresis, while DNA concentration and purity were determined using a NanoDrop One spectrophotometer (Thermo Fisher Scientific, MA, USA). PCR amplification (V3-V4 region) was performed using the extracted genomic DNA as the template with barcoded primers and Premix Taq (TaKaRa)

selected based on the target sequencing regions. The concentrations of the PCR products were analyzed using GeneTools Analysis Software (Version 4.03.05.0, SynGene), and equimolar amounts of each sample were pooled. The pooled PCR products were purified using the E.Z.N.A.® Gel Extraction Kit (Axygen Biosciences, CA, USA), with the target DNA fragments eluted in TE buffer. Library construction followed the standard protocol of the NEBNext® Ultra™ DNA Library Prep Kit for Illumina®. Sequencing was conducted on the Illumina MiSeq platform, generating raw image data files, which were processes via base calling to produce raw sequencing reads in FASTQ format. This format includes both nucleotide sequence information and corresponding quality scores. All procedures, including DNA extraction, PCR amplification, library construction, and high-throughput sequencing, were performed by Guangdong Magigene Biotechnology Co., Ltd. (Guangzhou, China). Genomic DNA was extracted with the TIANamp Bacteria DNA Kit (Tiangen, DP302). The 16S rRNA gene was amplified using universal primers 27F (5′-AGAGTTTGATCCTGGCTCAG-3′) and 1492R (5′-TACGGYTACCTTGTTACGACTT-3′). The qualify of the amplified sequences was assessed by agarose gel electrophoresis and sequenced by Hainan Nanshan Biotechnology Co., LTD, China..

Bioinformatic analysis for sequencing data

During sequencing data processing, paired-end raw reads underwent initial quality control using fastp (version 0.23.4), an ultra-fast all-in-one FASTQ preprocessor, applying sliding window quality trimming (https://github.com/OpenGene/fastp). Primer sequences were then removed using Cutadapt based on primer information at the sequence ends, generating paired-end clean reads (https://github.com/marcelm/cutadapt). These clean reads were subsequently merged using USEARCH's fastq_mergepairs function with default parameters, including a minimum overlap length of 16 bp and a maximum of 5 mismatches in the overlap region, to filter out non-conforming tags and obtain raw tags (http://www.drive5.com/usearch/). Finally, the raw tags underwent an additional round of quality control using fastp for sliding window quality trimming, yielding high-quality clean tags for downstream analysis (https://github.com/OpenGene/fastp). All sequences were conduced on

Magigene online cloud platform (cloud.magigene.com).

Isolation of cultivable bacteria from the rhizosphere of *S. trilobata*

Fresh rhizosphere soil of *S. trilobata* was suspended in 10 mL of sterile distilled water, vortexed for 2 minutes, and subjected to serial dilution (10^{-1} to 10^{-5}). Aliquots (100 µL) were spread onto LB agar plates and incubated at 30 °C for 48–72 hours. Morphologically distinct colonies were selected, purified through two rounds of subculturing, and stored in 20% glycerol at −80 °C.

Root exudate (RE) preparation and screening assay

Root exudates were prepared by rinsing intact root systems of *S. trilobata* three times with sterile distilled water, blotting the roots dry, and immediately grinding 5 g (fresh weight) in 20 mL of sterile distilled water using a pre-sterilized mortar and pestle. The resulting suspension was centrifuged at 12,000 × g at 4 °C for 15 minutes, and the supernatant was filtered sequentially through 0.22 µm sterile membrane filters twice to ensure sterility. Aliquots of the clarified root exudate were stored at −20 °C until further use. Overnight cultures of the bacterial isolates in LB broth were harvested by centrifugation, washed twice with sterile distilled water, and resuspended to an OD600 of 0.6–0.8. Each isolate was inoculated into 200 µL of LB medium supplemented with 20% clarified root exudate in a 96-well microplate, with an initial inoculum volume of 5 µL per well. LB medium supplemented with sterile distilled water was used as the control. The microplates were incubated at 30°C. The OD_{600} was measured every 2 hours until the growth curves reached a stable phase, indicating the end of exponential growth and the onset of stationary phase. This stable phase was characterized by minimal fluctuations in OD_{600} values, suggesting that the cultures had reached their maximum growth potential (K value). The duration of incubation varied among the isolates, ranging from 24 to 72 hours, depending on the growth characteristics of each strain. Isolates that exhibited an OD_{600} value at least 30% higher than that of the control at the stable phase were identified as root exudate-utilizing strains and selected for further analysis

Construction of the synthetic community

Based on the screening results, three Pseudomonas species and one Streptomyces species were selected for the construction of the synthetic community (SynCom). Each selected strain was cultured in LB broth until reaching the mid-logarithmic growth phase ($OD_{600} \approx 0.6$). The bacterial cells were then harvested by centrifugation at 8,000 × g for 5 minutes, washed twice with sterile distilled water, and resuspended to an OD_{600} of 0.8–1.0 (approximately 1×10^8 CFU mL^{-1}). Equal volumes of the four bacterial suspensions were subsequently combined to generate the final SynCom mixture, which was immediately used for plant inoculation experiments.

SynCom inoculation and plant growth assessment

Surface-sterilized *S. trilobata* stem cuttings, with initial lengths standardized to ensure uniformity, were rooted in sterile vermiculite for 7 days and then transplanted into trapezoidal pots (base dimension: 5 cm × 5 cm; top dimension: 7 cm × 7 cm; height: 8 cm). Prior to potting, all growth substrates were sieved through a 2-mm mesh to remove coarse debris and ensure textural homogeneity. The experiment consisted of three treatments. The fertile soil treatment (FS) was grown in autoclaved nutrient soil representing a nutrient-rich medium. The impoverished soil treatment (IS) was grown in autoclaved river sand soil without microbial inoculation, representing a nutrient-poor medium. The SynCom-amended treatment (IS+SynCom) was cultivated in the same autoclaved and sieved river sand soil and inoculated with 5 mL of the SynCom suspension applied directly to the root zone at transplantation. All plants were maintained in a growth chamber under controlled conditions (28°C, 16 h light/8 h dark photoperiod, 60% relative humidity). After a 3-day acclimation period, the inoculation procedure was repeated for the SynCom treatment group to reinforce microbial establishment. Plants were harvested 21 days after the final inoculation, and the following growth parameters were measured: root biomass, total biomass, root-to-shoot ratio, plant height, total leaf area, and specific leaf area (SLA).

Statistical analysis

Bacterial community α-diversity across different soil types was assessed using the

Kruskal-Wallis test based on operational taxonomic units (OTUs), with diversity indices including Chao1, Shannon, Simpson, and Pielou. The β-diversity was evaluated using non-metric multidimensional scaling (NMDS) based on Bray-Curtis dissimilarity matrices. To analyze correlations between soil samples and bacterial taxa, network analysis was performed on the top 20 OTUs at the order level, applying a threshold of r=0.5 and $p<0.05$. Differentially abundant taxa among groups were initially using the non-parametric Kruskal-Wallis rank-sum test, followed by the Wilcoxon rank-sum test to validate the consistency of differences across subgroups. Linear discriminant analysis (LDA) was used to estimate the effect size of species abundance on the observed differences. Functional prediction of bacterial communities was conduced using PICRUSt, normalizing OTU abundance to account for 16S rRNA gene copy numbers. OTUs were mapped to their corresponding Greengenes IDs and aligned with the COG database to infer associated functional categories. Bacterial growth data were subjected to one-way ANOVA to compare OD_{600} values among treatments at the stable phase of the growth curves. Significant differences between groups were further analyzed using post-hoc Tukey's HSD tests. A p-value of less than 0.05 was considered statistically significant. In the plant growth validation assay, growth parameters: total biomass, root biomass, root-shoot ratio, plant height, total leaf area and specific leaf area (SLA), were analyzed using two-way ANOVA to evaluate the main effects of soil type and inoculation treatment, as well as their interaction. Post-hoc Tukey's HSD tests were conducted to identify pairwise differences among treatment groups. Statistical significance was defined as $p < 0.05$. All statistical analyses were carried out using R software (version 4.3.0), with the assistance of the vegan, ggplot2, and agricolae packages.

Abbreviations

OTUs: Operational taxonomic units; NMDS: Non-metric Multidimensional Scaling LDA: Linear discriminate analysis; LEfSe: Linear discriminate analysis effect size; PICRUSt: Phylogenetic Investigation of Communities by Reconstruction of Unobserved States

Acknowledgements

Not applicable.

Authors' contributions

PL designed the research; GXL, Xl and XQ prepared the materials, XL, MZH and GYL analyzed the data, GXL, MZH and PL wrote and revised the manuscript. All authors read and approved the final manuscript.

Funding

This work was supported by Hainan Province key R&D Project (ZDYF2025XDNY122).

Availability of data and materials

The raw reads of 16S MiSeq data were deposited into the NCBI Sequencing Read Archive database (accession No. PRJNA1271135).

Ethics approval and consent to participate

Not applicable.

Consent for publication

Not applicable.

Declarations

The authors declare that they have no competing interests.

Clinical trial

Not applicable

References

1. Torres N, Herrera I, Fajardo L, Bustamante RO. Meta-analysis of the impact of plant invasions on soil microbial communities. BMC Ecol Evol. 2021;21:1-8.
2. Novoa A, González L, Moravcová L, Pyšek P. Effects of soil characteristics, allelopathy and frugivory on establishment of the invasive plant Carpobrotus edulis and a co-occuring native, Malcolmia littorea. PLoS One. 2012;7:e53166.
3. Callaway RM, Aschehoug ET. Invasive plants versus their new and old neighbors: a mechanism for exotic invasion. Science. 2000;290:521-23.
4. Qu T, Du X, Peng Y, Guo W, Zhao C, Losapio G. Invasive species allelopathy decreases plant growth and soil microbial activity. PloS one. 2021;16:e0246685.
5. Djurdjević, L, Mitrović M, Gajić G, Jarić S, Kostić O, Oberan L et al. An allelopathic investigation of the domination of the introduced invasive *Conyza canadensis* L. Flora. 2011:206:921-27.
6. Yuan Y, Wang B, Zhang S, Tang J, Tu C, Hu S et al. Enhanced allelopathy and competitive ability of invasive plant Solidago canadensis in its introduced range. J Plant Ecol 2013:6:253-63.
7. Zhou J, Xu Z, Zhong S, Yu Y, Xu Z, Du D et al. Nitrogen influence to the independent invasion and the co-Invasion of Solidago canadensis and Conyza canadensis via intensified allelopathy. Sustainability. 2022;14:11970.
8. Revillini D, David, AS, Reyes AL, Knecht LD, Vigo C, Allen P et al. Allelopathy-selected microbiomes mitigate chemical inhibition of plant performance. New Phytol. 2023;240:2007-19.
9. Mueller CW, Baumert V, Carminati A, Germon A, Holz M, Kögel-Knabner et al. From rhizosphere to detritusphere – Soil structure formation driven by plant roots and the interactions with soil biota. Soil Biol Biochem. 2024;193:109396
10. Berendsen RL, Pieterse CM, Bakker PA. The rhizosphere microbiome and plant health. Trends Plant Sci. 2012;17:478-86.
11. Niu H, Liu W, Wan F. Invasive effects of Ageratina adenophora Sprengel (Asteraceae) on soil microbial community and physical and chemical properties. Acta Ecol. 2007;Sin 27:3051-60.
12. Zhang P, Li B, Wu J, Hu S. Invasive plants differentially affect soil biota through

litter and rhizosphere pathways: a meta-analysis. Ecol Lett. 2019;22:200-10.
13. Liu B, Yan J, Li W, Yin L, Li P, Yu H et al. Mikania micrantha genome provides insights into the molecular mechanism of rapid growth. Nat Commun. 2020;11, 340.
14. Cai M, Huang J, Chen M, Chen L, Zhang X, Chen M et al. The role and synthesis mechanism of anthocyanins in Sphagneticola trilobata stems under low temperature. Biol Invasions. 2024;26:2851-67.
15. Yan X, Liu Q, Shou H, Zeng X, Zhang Y, Chen L et al. The categorization and analysis on the geographic distribution patterns of Chinese alien invasive plants. Biodiversity Science. 2014;22:667-76.
16. Ullah MS, Sun J, Rutherford S, Ullah I, Javed Q, Rasool G et al. Evaluation of the allelopathic effects of leachate from an invasive species (Wedelia triobata) on its own growth and performance and those of a native congener (W. chinensis). Biol Invasions. 2021;23:3135-49.
17. Zhang W, Damm U, Crous PW, Groenewald JZ, Niu X, Lin J et al. Anthracnose Disease of Carpetgrass (*Axonopus compressus*) Caused by Colletotrichum hainanense sp. nov. Plant Dis. 2020;104:1744-50.
18. Xiong Y, Wei Z, Liu J, Li J, Jian S, Zhang X et al. Shoot propagation, regeneration, and callus induction and differentiation, of *Axonopus compressus* (Swartz) Beauv. In Vitro Cell. Dev. Biol. Plant. 2024;60:478-86.
19. Ling N, Wang T, Kuzyakov Y. Rhizosphere bacteriome structure and functions. Nat Commun. 2022;13:836.
20. Spain AM, Krumholz LR, Elshahed MS. Abundance, composition, diversity and novelty of soil Proteobacteria. ISME J. 2009;3:992-1000.
21. Jones RT, Robeson MS, Lauber CL, Hamady M, Knight R, Fierer N. A comprehensive survey of soil acidobacterial diversity using pyrosequencing and clone library analyses. ISME J. 2009;3:442-53.
22. Navarrete AA, Kuramae EE, de Hollander M, Pijl AS, van Veen JA, Tsai SM. Acidobacterial community responses to agricultural management of soybean in Amazon forest soils. FEMS Microbiol Ecol. 2013;8:607-21.
23. Tang F, Wang L, Fu M, Huang N, Li W, Song W. Spatio-temporal pattern evolution

612 and regulatory zoning of suitability for farmland scale utilization in China based on
613 multi-source data. Ecol Indic. 2024;166:112475.
614 24. Fahde S, Boughribil S, Sijilmassi B, Amri A. Rhizobia: a promising source of plant
615 growth-promoting molecules and their non-legume interactions: examining
616 applications and mechanisms. Agriculture. 2023;13:1279.
617 25. Naqqash T, Malik KA, Imran A, Hameed S, Shahid M, Hanif MK et al. Isolation
618 and characterization of Rhizobium from non-leguminous potato plants: New
619 frontiers in Rhizobium research. Biol Fert Soils. 2024;60(3):307-25.
620 26. Liu Y, Pei T, Du J, Huang H, Deng MR, Zhu H. Comparative genomic analysis of
621 the genus Novosphingobium and the description of two novel species
622 *Novosphingobium aerophilum* sp. nov. and *Novosphingobium jiangmenense* sp. nov.
623 Syst. Appl. Microbiol. 2021;44(3):126202. .
624 27. Xie X, Chen Y, Bu Y, Dai C. A review of allelopathic researches on phenolic
625 acids. Acta Ecol Sin. 2014;34:6417-28.
626 28. Chen Q, Wu W, Qi S, Cheng H, Li Q, Ran Q et al. Arbuscular mycorrhizal fungi
627 improve the growth and disease resistance of the invasive plant *Wedelia trilobata*. J
628 Appl Microbiol. 2021;130(2):582-91.
629 29. Mei Y, Li X, Zhou J, Kong F, Qi S, Zhu B et al. Both adaptability and endophytic
630 bacteria are linked to the functional traits in the invasive clonal plant Wedelia
631 trilobata. Plants. 2022;11(23):3369.
632 30. Kim JS, Dungan RS, Crowley D. Microarray analysis of bacterial diversity and
633 distribution in aggregates from a desert agricultural soil. Biol Fert Soils. 2008;
634 44:1003-11.
635 31. Neilson JW, Califf K, Cardona C, Copeland A, Van Treuren W, Josephson W, J.
636 Significant impacts of increasing aridity on the arid soil microbiome. mSystems.
637 2017;2:10-1128.
638 32. Gong X, Xu L, Langwig M V, Chen Z, Huang S, Zhao D et al. Globally distributed
639 marine Gemmatimonadota have unique genomic potentials. MICROBIOME.
640 2024;12: 149.
641 33. Liu Y, Huang W, Yang Q, Zheng Y, Li S, Wu H et al. Research advances of plant

invasion ecology over the past 10 years. Biodiversity Science. 2022;30:22438.
34. Yu H, Han C, Ren G, Wu X, Qi S, Yang B et al. Heat Wave Adaptations: Unraveling the Competitive Dynamics Between Invasive Wedelia trilobata and Native Wedelia chinensis. Plants. 2024;13:3480.
35. Banerjee S, Schlaeppi K, van der Heijden M.G.A. Keystone taxa as drivers of microbiome structure and functioning. Nat Rev Microbiol. 2018;16:567-76
36. Dutta S, Islam Z, Das S,Barman A,Chowdhury M,Prasad B et al. Harmonizing plant resilience: unveiling the symphony of membrane lipid dynamics in response to abiotic stresses: a review. Discov. Plants. 2025;2:61.
37. Cui K , Xu T, Chen J, Yang H, Liu X, Zhuo R et al. Siderophores, a potential phosphate solubilizer from the endophyte Streptomyces sp. CoT10, improved phosphorus mobilization for host plant growth and rhizosphere modulation. J CLEAN PROD. 2022;367:133110.
38. Poorter H, Nagel O. The role of biomass allocation in the growth response of plants to different levels of light, CO2, nutrients and water: a quantitative review. FUNCT PLANT BIOL. 2000;27:1191-91.
39. Wright IJ, Reich PB, Westoby M, Ackerly DD, Baruch Z, Bongers F et al. The worldwide leaf economics spectrum. Nature. 2004;428: 821-27.
40. Silva MC, Carvalho AJ, Lima JD, Carvalho R, Oliveira HG. Beneficial effects of ACC deaminase-producing rhizobacteria on the drought stress resistance of Coffea arabica L. Plants. 2025;14: 2251.

Supplementary Files

This is a list of supplementary files associated with this preprint. Click to download.

- TableS1.docx
- SupplementaryInformation.docx
- FigureS1.tif
- FigureS3.tif
- FigureS4.tif
- FigureS2.tif